AADE-17-NTCE-63

Effect of Temperature on Casing and Drillstring Stretch Calculations

Samuel Ighalo and Yousuf Mazhar, Halliburton

Abstract

An estimation of casing stretch when run in the hole is necessary for depth correction purposes and adequate space outs. Total stretch in the pipe during well operations is the sum of stretch attributed to axial load, buckling, ballooning, and temperature effects. Stretch resulting from temperature effects can generate significant errors in total stretch calculation if not properly taken into account. The default assumption is to use the geothermal gradient for thermal stretch; however, results show that using a geothermal temperature profile for calculating stretch overestimates the actual stretch in the wellbore.

This paper presents a study that simulated the sequences of operations to obtain actual wellbore temperature profiles. Simulated wellbore temperatures were used as inputs in a torque-and-drag simulator to estimate the total stretch, including the thermal component. Another case calculated the total stretch by eliminating the thermal effect. Two field cases from a deepwater well in the Gulf of Mexico were used for validation.

The predictions showed good agreement with the available field measurements using the simulated temperature model. Conversely, stretch based on the geothermal temperature profile differed from actual field measurements. The geothermal temperature model approximates a linear temperature profile across the liner section when, in reality, the temperature profile is nonlinear. This paper shows that using a simulated temperature profile that models actual wellbore conditions yields much higher accuracy compared to the geothermal temperature profile.

Introduction

As wells reach greater depths, the importance of determining the actual length of casings and drillstrings when run in the hole has increased. In deepwater environments, it is often challenging to measure these lengths because the pipe undergoes significant stretch resulting from its own weight, ballooning, buckling, and temperature. It is good practice to accurately measure stretch on the rig for depth correction purposes, as well as for other critical well operations that rely on such measurements. To develop reliable predictive tools, measurements in the field should match models developed based on the bottomhole assembly (BHA), drilling fluids, and operations planned for the hole section or the well. When the specific details of drilling and cementing operations are unknown, simulation of the well construction process based on realistic assumptions can provide an “order of magnitude” analysis.

The presence of drillpipe, circulation of the drilling mud, and friction between the drillstring and the wellbore can result in the temperature distribution[1] being different from the undisturbed geothermal temperature. Casing initial temperature is assumed to be the prevailing geothermal undisturbed temperature gradient because of its simplicity[2]. The drilling process is subject to many operational parameters, which are difficult to quantify or predict[2]. The general calculation for the incremental axial load caused by changes between initial and final string states includes strain components for mechanical displacement, temperature change, ballooning, and buckling. The severity of thermal loads is a direct function of the difference between initial and final average casing temperature across its free length.

It is believed that using the geothermal temperature of a well overestimates the stretch of the casing and drillstrings. API circulating temperature tends to overestimate the circulating temperature when casing is in the hole. This, in turn, leads to over-retardation, which then leads to excessive waiting-on-cement (WOC) time. It is essential to estimate accurate wellbore temperatures by taking into account the sequence of operational events during the drilling of the well sections.

This study determines the predicted wellbore temperatures for 16- and 14-in. intermediate liners during drilling operations and then uses the output for torque-and-drag simulation to estimate stretch. An alternative approach is to eliminate the stretch thermal component for modeling stretch in casings and drillstrings. In general, the approach involves performing thermal simulations of the planned drilling, casing runs, and cementing operations to determine the thermal profile of the well. These outputs are used to determine the thermal component of the stretch calculation. Two case studies are used in this study to ascertain the feasibility of eliminating the thermal component from the stretch equation. By eliminating the thermal component of the stretch, the modeling only considers the mechanical stretch. Another option is to include the thermal component by using the output obtained through simulating the operational events in the wellbore.

Stretch in Tubulars

Pipe length is modified in a downhole environment by mechanical stretch resulting from gravity, thermal expansion, and the hydrostatic pressure of the mud column. During circulation, the high pressures within the pipe cause additional elongation, and annular fluid friction against the pipe wall also affects the length. When drilling, the amount of mechanical stretch is modified as the tension changes with varying weight on bit.

The total stretch in the pipe is given by the following equation[5]:

$$\Delta L_{stretch} = \Delta L_{Hlaw} + \Delta L_{buck} + \Delta L_{balloon} + \Delta L_{temp} \qquad (1)$$

Where ΔL_{Hlaw} is the stretch caused by self-weight (Hooke's law), ΔL_{buck} is the result from buckling, $\Delta L_{balloon}$ is caused by ballooning, and ΔL_{temp} is the effect of temperature. **Table 1** shows the different stretch components that make up the total stretch and their formulas.

Table 1: Stretch Equations for Well Tubulars

Stretch Component	Equations
Self-weight	$\Delta L_{Hlaw} = \frac{F_{apa} L_c}{A_c E} + \frac{\Delta F_{apa} L_c}{2 A_c E}$
Buckling	$\Delta L_{buck} = \frac{r_{cl}^2 F_{apa} L_c}{4EI} + \frac{r_{cl}^2 \Delta F_{apa} L_c}{8EI}$
Ballooning	$\Delta L_{balloon} = \frac{-v L_c}{E\left[\left(\frac{d_{bo}}{d_{bi}}\right)^2 - 1\right]} \, x \left[\left(\rho_{mi} - \left(\frac{d_{bo}}{d_{bi}}\right)^2 \rho_{ma}\right) L_c + 2\left(P_s - \rho_{ma}\left(\frac{d_{bo}}{d_{bi}}\right)^2\right)\right]$
Thermal	$\Delta L_{temp} = \propto L_c \Delta T$

Stretch results from a combination of temperature increases, self-weight, ballooning, and buoyancy; typically, temperature increase is the most important. Stretch reduces with drag and therefore varies with completion fluid and mud type. Stretch does not vary with pipe thickness or diameter; so, in the absence of drag, it does not vary between tubing and casing. Stretch is nonlinear (doubling the length of pipe typically quadruples the stretch). Stretch in excess of 20 ft has been observed in deepwater wells, which is quite significant and should not be ignored.

Tallies can be inaccurate, for example, if a joint is rejected but not recorded or errors in a spreadsheet go unnoticed[3]. Pipe stretch is significant in highly deviated wells and in deep vertical well. Matching stretch with actual field measurements is therefore dependent on the operation mode. As an example, setting a packer in the well involves rotating off bottom mode of operation or tripping in the hole. Running in casing can also involve different modes of operation. Care should be taken to accurately model the modes of operation that the wellbore undergoes. Estimating stretch using commercial torque-and-drag simulators can produce mixed results when compared to field data. It is believed deviations from actual stretch values are caused primarily by thermal stretch. Thermal stretch needs to be modeled correctly using a thermal simulator to estimate the correct temperature profile during the drilling operational sequences.

Fig. 1 shows a graphical representation of the different temperature profiles that can occur in a normal drilling scenario.

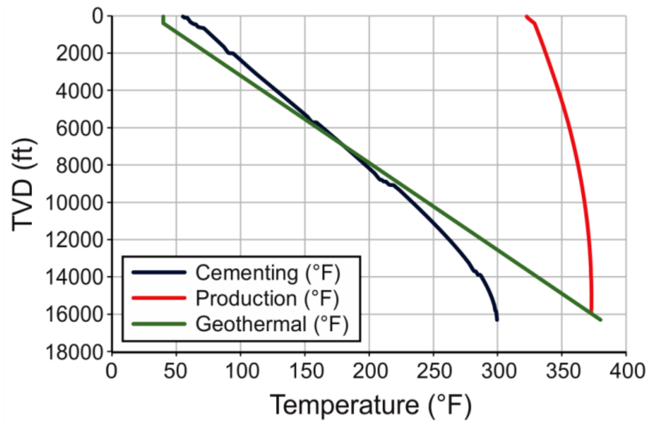

Figure 1: Temperature profiles for different wellbore scenarios

Axial pipe movement causes elongation or shortening resulting from wall friction and, in some cases, buckling can occur. As discussed in this paper, the major factors affecting casing/drillstring length are those caused by stretch resulting from self-weight in the drillstring and thermal expansion. A commercial torque-and-drag simulator was used to calculate the stretch of casing/drillstring using temperature inputs from the thermal studies performed. The torque-and-drag model used was the soft string, which was considered sufficient for modeling a running-in-hole (RIH) scenario.

In the soft string model, the workstring is treated as an extensible cable with zero bending stiffness. It assumes that the pipe is always positioned at the center of the hole and the workstring is assumed to be contacting the wellbore for the entire length in a deviated section of hole. Conversely, the stiff string model computes the additional side force from stiff tubulars bending in a curved hole, as well as the reduced side forces from pipe straightening caused by pipe/hole clearance. The stiff string model was not considered in this study.

Thermal Modeling and Stretch Analysis

The key features for wellbore simulation are transient effects, flowing fluids, wellbore geometry, and flow options[4]. Drilling, cementing, fracturing, and production startup are all transient operations, where fluid temperatures can change approximately 100°F or more in a matter of minutes during flow in the well.

Temperature-dependent properties and wall coefficients need to be updated as the temperatures and rheological properties change with time and depth. The viscosity of drilling muds changes with temperature during circulation. The geometry determines the cross-sectional flow area and the fluid velocity, which in turn governs heat transfer. Temperatures during liner cementing are significantly influenced by the size of the liner and annular clearance.

For this study, thermal analysis was performed using a commercial thermal simulator. Extensive simulations of the drilling operational sequences were performed to obtain the thermal history of 14- and 16-in. liner sections of the well. The obtained results constitute the predicted wellbore temperature profile while running the casing in hole.

Two temperature models were simulated. The first case was a RIH scenario that modeled a tripping-in event and circulation after reaching the hole section total depth (TD). The second case was a cementing scenario (start of WOC) that modeled circulation followed by a static condition. The RIH scenario showed a higher temperature gradient because it occurred immediately after a drilling event; the drilling process disturbs the wellbore, heating the upper sections and cooling the lower sections.

The start of WOC scenario showed a moderate to near constant temperature gradient, where temperature at the upper section of the casing was almost the same as the lower section. However, the geothermal temperature profile showed a much higher temperature gradient than the other profiles. To simplify calculations, another case was analyzed that eliminated the thermal component of stretch, and it showed a good match with actual stretch data, which were also consistent during the entire study.

Simulation of Wellbore Temperatures

To model the desired casing/liner temperatures for the two scenarios, drilling operations before RIH and the start of WOC were simulated. Simulation of previous drilling operations in sequential order helps to accurately track the well temperature history, which was used to determine the initial temperatures for the desired operations.

For this study, simulations were performed beginning with the drilling of a 26-in. hole section, followed by running 22-in. casing and then cementing operations. Other operations, simulated in sequence, included tripping-in an 18 1/8-in. × 21-in. BHA, drilling of an 18 1/8-in. × 21-in. section, running a 16-in. liner, and cementing the 16-in. liner. Subsequently, tripping-in and drilling operations were simulated for a 14-in. × 16 1/2-in. section followed by running a 14-in. liner and cementing the 14-in. liner. **Fig. 2** shows simulated thermal profiles for all of these operations.

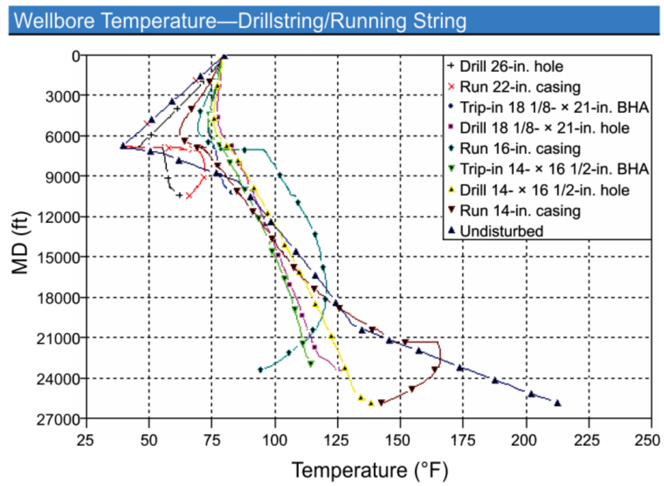

Figure 2: Simulated thermal profiles for drilling operational sequences up to running 14-in. casing

Stretch was calculated based on two separate thermal profiles for both 16- and 14-in. liners. The first calculation was based on the temperature of both liners after RIH, and the second was determined for the start of WOC. **Figs. 3 and 4** show temperatures for the 16-in. liner after RIH and the start of WOC, respectively.

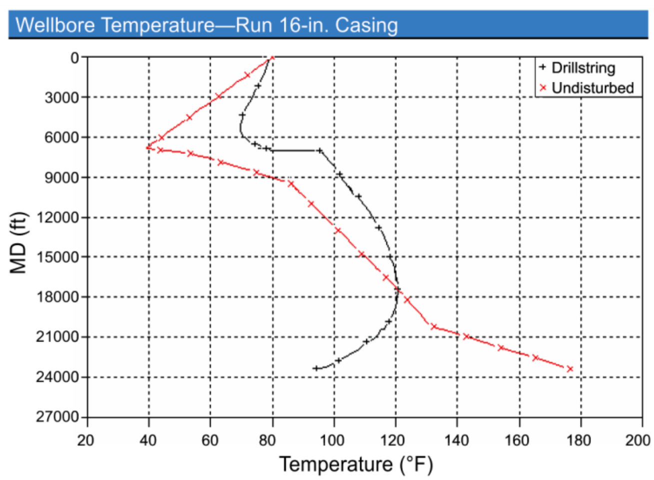

Figure 3: RIH temperature for 16-in. liner

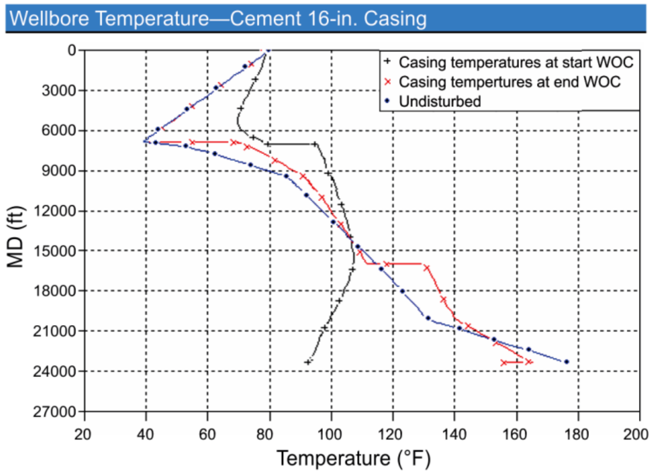

Figure 4: Start of WOC temperature for 16-in. liner

Similarly, **Figs. 5 and 6** show temperatures profiles for the 14-in. liner after RIH and at start of WOC, respectively.

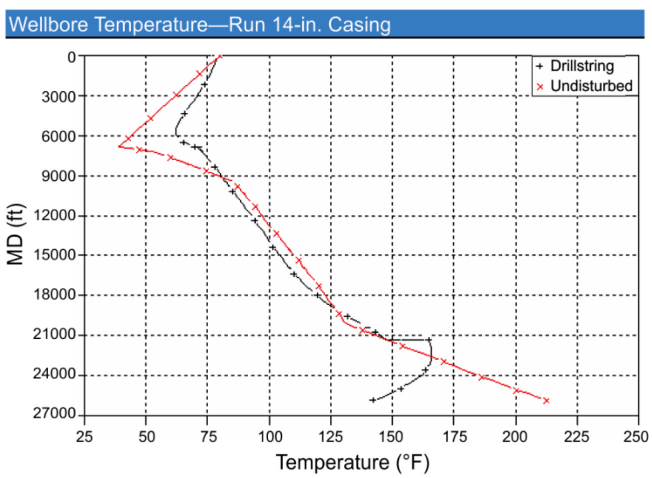

Figure 5: RIH temperature for the 14-in. liner

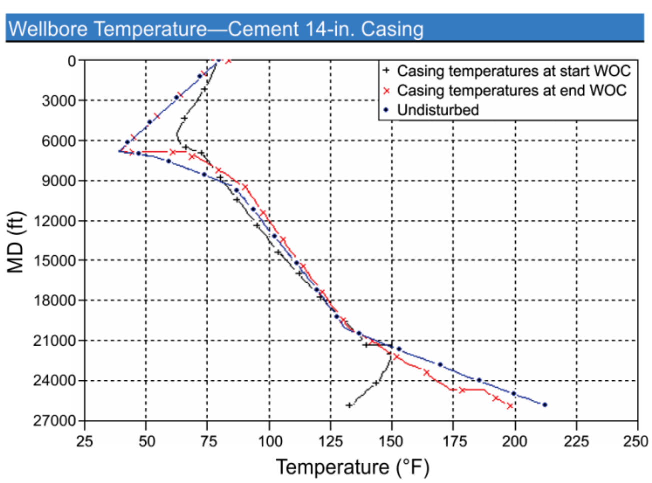

Figure 6: Start of WOC for the 14-in. liner

The thermal profiles shown in **Figs. 5 and 6** indicate that the RIH and cementing temperatures were slightly different. The RIH case simulated a hole condition where circulation occurred after tripping-in; thus, liner strings were relatively cooler at the bottom compared to the temperature at the start of WOC.

Field Examples

A well located in deepwater Gulf of Mexico, off the coast of Louisiana, had a TD of approximately 30,000 ft measured depth (MD). It was an S-shaped well with a 16-in. liner shoe placed at a maximum inclination of approximately 30°, and a 14-in. shoe was placed in a drop section at an approximate 10° inclination. Actual stretch was measured on the rig for both liners, which was compared with the simulated stretch calculated by torque-and-drag software based on different temperature profiles.

Case I: 16-in. Liner Analysis and Results

Thermal simulations were performed for the 16-in. liner, and two temperature profiles for RIH **(Fig. 3)** and the start of WOC **(Fig. 4)** were considered for calculating stretch. When analysis was performed with the liner RIH temperature profile, stretch in the landing string caused by the 16-in. liner was 19.2 ft. For the start of WOC temperature profile, the resulting calculation yielded a stretch value of 18.8 ft.

The study also investigated a case eliminating the thermal effect from stretch calculations by assuming the thermal expansion coefficient was zero for the complete liner string. This resulted in a stretch of 18.0 ft for the 16-in. liner. For comparison purposes, another analysis was performed using the geothermal temperature profile that resulted in a stretch of 28.5 ft, which was considerably higher than the other thermal models. All of these simulation results were compared with actual measured stretch on the rig (17 ft). **Fig. 7** compares stretch results calculated based on different thermal assumptions to actual measured stretch for the 16-in. liner.

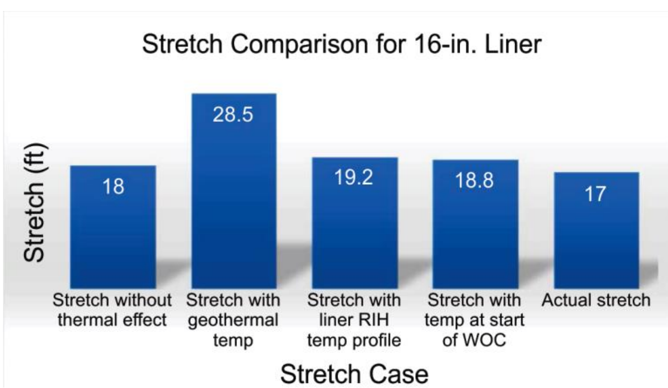

Figure 7: Stretch comparison for 16-in. liner

Based on these results, it can be observed that stretch estimated based on the temperature profile at the start of WOC was much closer to the actual measured stretch compared to the liner RIH thermal profile. The thermal profile at the start of WOC showed the upper and lower casing section temperatures were closer, resulting in a small thermal gradient compared to RIH thermal profile. Analysis performed without the thermal effect or with a zero thermal gradient assumption provided the best stretch results with the least percentage of error compared to other cases. Stretch based on the geothermal profile that had the highest thermal gradient provided the highest margin of error. **Fig. 8** compares the percentage of error between all four cases for the 16-in. liner.

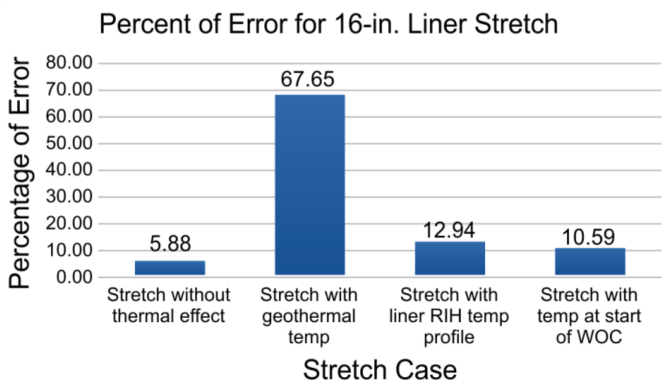

Figure 8: Percentage of error for 16-in. liner stretch

Case II: 14-in. Liner Analysis and Results

A similar methodology was used to analyze the 14-in. liner stretch. First, analysis was performed using the 14-in. liner RIH temperature profile, resulting in 18.1 ft of stretch in the landing string. Another case was studied using the same inputs but changing the thermal profile to temperature at the start of WOC. This resulted in a stretch of 16.9 ft at the surface. Analysis performed eliminating the thermal effect from the equation resulted in 16.6 ft of stretch. The geothermal temperature-based stretch estimation resulted in 32.2 ft of stretch. While running the 14-in. liner at the rig, the actual measured stretch was recorded at approximately 16.0 ft. **Fig. 9** compares the stretch results for the simulated temperatures.

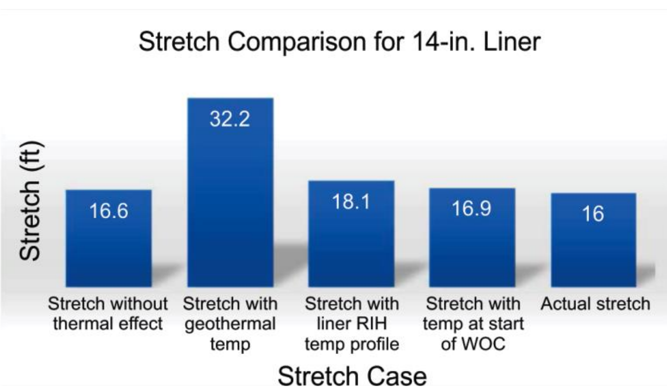

Figure 9: Stretch comparison for 14-in. liner

Similar to the results for the 16-in. liner, stretch estimated for the 14-in. liner based on the temperature profile at the start of WOC was closer to the actual measured stretch compared to the liner RIH thermal profile. Furthermore, analysis performed without the thermal effect or with a zero thermal gradient assumption provided much closer stretch results, similar to those from the 16-in. liner. As expected, stretch based on the geothermal gradient yielded the highest margin of error. **Fig. 10** compares the percentage of error between all four cases for the 14-in. liner.

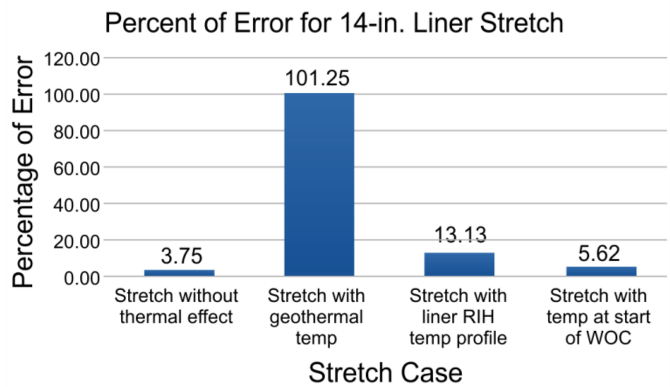

Figure 10: Percentage of error for 14-in. liner stretch

Discussion

Simulation results showed that the start of WOC temperature model (cementing temperature) was in good agreement with the actual stretch, with an approximate 10% margin of error. The RIH temperature model provided a margin of error just under 15%, as it had a relatively higher gradient than the cementing temperature. The worst results were observed when using the geothermal temperature profile. Based on these findings, simulating actual drilling operations is beneficial because it provides good agreement with actual stretch values. Additionally, using the geothermal gradient can result in erroneous stretch results. This study also showed that eliminating the thermal effect based on the assumption that the temperature of upper and lower casing sections is similar and the temperature gradient is almost zero is reasonable for modeling purposes.

Conclusions

The predictions show good agreement with the available field measurements using the simulated temperature model. The maximum difference in simulated thermal cases was less than 15%, which, in terms of length, represented approximately 2 ft. In deepwater wells with total depths greater than 25,000 ft MD, this difference can be negligible. However, stretch calculated based on the geothermal temperature profile was remarkably different compared to actual field measurements. The geothermal temperature model approximates a linear temperature profile across the liner section, when, in reality, the temperature profile is nonlinear.

The nonlinear nature of the actual wellbore temperature is caused by the dynamic wellbore conditions occurring during drilling operations. However, stretch calculated without the thermal effect and assuming a negligible change in temperature yielded much closer results to the simulated temperature model and actual field measurements.

In general, this study demonstrates the importance of using the appropriate temperature model for predicting actual stretch in a wellbore. Using an alternate temperature profile that models actual wellbore conditions provides much higher accuracy compared to a geothermal temperature profile. For simplicity, the assumption of a negligible change in temperature can also provide reasonable results that are in good agreement with the actual stretch of casing strings and can be used for future wells.

Acknowledgments

The authors thank Halliburton for permission to publish this paper.

Nomenclature

$\propto$	= *coefficient of linear thermal expansion*
$\Delta L_{balloon}$	= *stretch resulting from ballooning*
ΔL_{buck}	= *stretch resulting from buckling*
ΔL_{Hlaw}	= *stretch resulting from axial load*
$\Delta L_{stretch}$	= *total stretch*
ΔL_{temp}	= *stretch resulting from temperature effects*
ΔT	= *temperature change over component length*
A_c	= *cross-sectional area of component*
BHA	= *bottomhole assembly*
d_{bi}	= *inside diameter of body*
d_{bo}	= *outside diameter of body*
F_{apa}	= *axial force as calculated by the pressure area method*
E	= *Young's modulus of elasticity*
I	= *moment of inertia*
L_c	= *length of component*
MD	= *measured depth*
ρ_{ma}	= *mud density in annulus at depth of string component*
ρ_{mi}	= *mud density inside string component*
p_s	= *surface pressure, string side*
r_{cl}	= *radial clearance between wellbore and string*
RIH	= *run in hole*
TD	= *total depth*
v	= *Poisson's ratio for component*
WOC	= *waiting on cement*

References

1. Dashevskiy, D., Dahl, T., Brooks, A. G., Zurcher, D., Lofts, J. C., and Dankers, S. 2006. Dynamic Depth Correction To Reduce Depth Uncertainty and Improve MWD/LWD Log Quality. Presented at the SPE Annual Technical Conference and Exhibition, San Antonio, Texas, USA, 24–27 September. SPE-103094-MS. http://dx.doi.org/10.2118/103094-MS.
2. McSpadden, A.R. and Glover, S. 2008. Importance of Predicted Cementing Temperatures for Critical HP/HT Casing Design: Guidelines and Case Studies. Presented at the SPE Annual Technical Conference and Exhibition, Denver, Colorado, USA, 21–24 September. SPE-114928-MS. http://dx.doi.org/10.2118/114928-MS.
3. Bellarby, J. 2009. *Well Completion Design*. 1st Edition. Amsterdam: Elsevier.
4. Mitchell, R.F. and Wedelich III, H.F. 1989. Prediction of Downhole Temperatures Can Be Key for Optimal Wellbore Design. Presented at the SPE Production Operations Symposium, Oklahoma City, Oklahoma, USA, 13–14 March. SPE-18900-MS. http://dx.doi.org/10.2118/18900-MS.
5. Halliburton. 2013. *WELLPLAN Manual*. Houston, Texas: Halliburton.